

12th Joint MMM/Intermag Conference

January 14-18, 2013, Chicago, Illinois, USA

[Conference Details](#)

[Information for Contributors](#)

[Information for Students](#)

[Travel Information](#)

[About MMM](#)



12th Joint MMM 2013
Chicago, Illinois

Who should attend

The 12th Joint MMM/Intermag Conference will be held in the heart of Chicago, Illinois, easily accessible from O'Hare and Midway Airports. Members of the international scientific and engineering communities interested in recent developments in fundamental and applied magnetism are invited to attend the Conference and contribute to its technical sessions.

Advance Registration is now closed. On-site Registration will be open at 4:00 PM on January 14th in the Regency Foyer on the Gold Level of the Chicago Hyatt Regency.

To reserve a hotel room for the conference, [click here](#). Please note that the student rate room block has now sold out.

To see the conference program "at a glance," including symposia, invited speakers, and special sessions, please [click here](#).

» If you will need a US visa to travel to the conference, please click [here](#) for important information.

**12th Joint MMM/
Intermag Program**

Itinerary Planner

Abstracts Book

iPhone / iPad app

CHICAGO

Few cities in the world can match the character and culture of Chicago. Here, you can find world-class dining, museums and entertainment. Chicago is the largest and most visited city in the Midwest of the United States.

As the official Chicago visitors' site, the Chicago Convention & Tourism Bureau is dedicated to helping you figure out what to do in Chicago during your stay. On their web site, www.choosechicago.com you can experience the city like a local by obtaining the latest information on Chicago attractions such as the Navy Pier and Millennium Park, as well as the numerous outstanding museums and galleries. Most of these, including the world-renowned Art Institute of Chicago, are easily accessible from the conference hotel by walking or through Chicago's easy-to-use public transportation system. At the web site, you can also learn all about where to eat in Chicago – from famous pizza joints to upscale restaurants. The site also offers a complimentary Visitors' Guide and suggested itineraries for seeing the city, as well as weekly weather updates. So join us at the 2013 Joint Conference and experience a new city.



Please join us for the 12th Joint MMM/Intermag, 2013, Chicago
(Photo Credit: ©Chicago Convention & Tourism Bureau)

Important Note about Visas...

If you plan to submit an abstract and/or attend the 12th Joint MMM/Intermag Conference, please make an appointment now to apply for your visa to the U.S. This application process may take 3-6 months, so we urge you to submit your application now.

IMPORTANT DATES

Abstract submission opens
11 July 2012

Abstract submission closes
3 August 2012

Accept / reject notices
5 Sept 2012

Manuscript submission opens
24 Sept 2012

Manuscript submission closes
9 Nov 2012

Student travel award deadline
5 Oct 2012

Conference registration closes
17 Dec 2012

Hotel reservation deadline
17 Dec 2012

DR-06. Magnetically Induced Vibration of an IPM motor Due to the Distorted Magnetic Force Originating from the Flux Weakening Control. D. Kim¹, G. Jang¹ and J. Nam¹. *PREM, Dept. of Mechanical Engineering, Hanyang University, Seoul, Republic of Korea*

DR-07. A New Topology of Coaxial Magnetic Gear Using Stationary Permanent Magnet Ring. X. Li¹, K. Chau², M. Cheng¹, W. Hua¹ and Y. Du¹. *1. School of Electrical Engineering, Southeast University, Nanjing, Jiangsu, China; 2. Department of Electrical and Electronic Engineering, The University of Hong Kong, China*

DR-08. Proximity Losses in the Windings of High Speed Brushless Permanent Magnet AC Motors with Single Tooth Windings and Parallel Paths. M. Popescu² and D. Dorrell¹. *1. University of Technology Sydney, Sydney, NSW, Australia; 2. Motor Design Ltd., Elleseme, United Kingdom*

DR-09. Thermal Analysis of Water Cooled IPMSM Using Thermal Equivalent Circuit. K. Kim¹, B. Lee¹, J. Jung¹ and J. Hong¹. *Automotive Engineering, Hanyang University, Seoul, Republic of Korea*

DR-10. Cooling Optimization of a High Speed Permanent Magnet Synchronous Motor. J. Dong¹, Y. Huang¹ and L. Jin¹. *School of Electrical Engineering, Southeast University, Nanjing, Jiangsu, China*

WEDNESDAY
AFTERNOON
1:00

RIVERSIDE CENTER

Session DS

PATTERNED FILMS AND NANOPARTICLES II: VORTICES, NANOWIRES, AND MAGNETIC MEDIA (POSTER SESSION) Randy Dumas, Chair

DS-01. Lateral Interactions of Magnetic Domain Walls Analyzed by Magnetic Force Microscopy. C. Nam^{1,2}, M. Mascaro¹ and C. Ross¹. *1. Materials Science and Engineering, MIT, Cambridge, MA; 2. Physics, Hannam University, Daejeon, Republic of Korea*

DS-02. Vortex state formation and stability in single and double layer arrays of nanorings and nanodisks. M. Zhu¹, C. Mathieu¹, S. Dubbaka¹ and W. Scholz¹. *Seagate Technology, Bloomington, MN*

DS-03. Probing the magnetization reversal of permalloy nanorings with high wall height-to-thickness ratios. Y. Huang¹, C. Chao², C. Kuo², L. Horng² and J. Wu^{1,2}. *1. Graduate Institute of Photonics, National Changhua University of Education, Changhua, Taiwan; 2. Department of Physics, National Changhua University of Education, Changhua, Taiwan*

DS-04. Influence of asymmetric degree on vortex state and switching fields in Permalloy rings. C. Huang¹, W. Lin², K. Hu¹, T. Wu¹, J. Wu¹ and L. Horng¹. *1. Department of Physics and Taiwan SPIN Research Center, National Changhua University of Education, Changhua, Taiwan; 2. Institute of Photonics, National Changhua University of Education, Changhua, Taiwan; 3. Department of Electronic Engineering, National Formosa University, Yunlin, Taiwan*

DS-05. Magnetic Reversal Mechanism in Dome-Like Nanostructures. J.L. Palma¹, C. Gallardo¹, J. Escrig^{1,2} and J.C. Denardin^{1,2}. *1. Physics Department, Universidad de Santiago de Chile (USACH), Santiago, Chile; 2. Center for the Development of Nanoscience and Nanotechnology (CEDENNA), Santiago, Chile*

DS-06. Enhanced magnetic anisotropy of Metal-Organic nanowire arrays by FeCu/ polypyrrole co-electrodeposition. X. Luo¹, S. Tang¹, Y. Li¹, W. Xia¹, J. Gao¹, S. Zhang¹ and Y. Du¹. *Nanjing National Laboratory of Microstructures, Jiangsu Provincial Laboratory for Nanotechnology and Department of Physics, Nanjing University, Nanjing, Jiangsu, China*

DS-07. Transport Properties of Magnetic Ni and Ni-alloy Nanowire Arrays. D.C. Leitao¹, L.G. Vivas¹, C.T. Sousa², A.M. Pereira², M. Vazquez², J. Ventura² and J.P. Araujo². *1. INESC-MN, Lisboa, Portugal; 2. IFIMUP-IN, Porto, Portugal; 3. ICMN - CSIC, Madrid, Spain*

DS-08. Magnetic field angle dependence of the magnetization reversal in cylindrically distributed nanowires arrays with longitudinal and transversal anisotropy. C. Garcia^{1,2}, V. Vega², V. Prida², P. Vargas³ and C.A. Ross⁴. *1. Physics, Bogazici University, Istanbul, Turkey; 2. Física, Universidad de Oviedo, Oviedo, Spain; 3. Física, Universidad Tecnica Federico Santa Maria, Valparaíso, Chile; 4. Materials Science and Engineering, MIT, Cambridge, MA*

DS-09. Tailoring magnetic anisotropy in Co_{100-x}Ni_x nanowire arrays. A. Pereira^{1,4}, C. Gallardo^{2,4}, J. Briones^{2,4}, L. Gonzalez Vivas³, J. Denardin^{2,4} and J. Escrig^{2,4}. *1. Metalurgia, Universidad de Santiago de Chile, Santiago, Santiago, Chile; 2. Física, Universidad de Santiago de Chile, Santiago, Santiago, Chile; 3. Institute of Materials Science of Madrid, Madrid, Madrid, Spain; 4. Center for the Development of Nanoscience and Nanotechnology at Santiago, Santiago, Chile*

DS-10. Structural and magnetic properties of patterned perpendicular media with linearly graded anisotropy. J. Zhang¹, Z. Sun², J. Sun¹, D. Li² and S. Kang¹. *1. Physics, Shandong University, Jinan, Shandong, China; 2. MINT Center, The University of Alabama, Tuscaloosa, AL*

DS-11. Energy barrier versus switching field for patterned Co₉₀Pt₁₀ alloy and Co/Pt multilayer films. J. de Vries¹, T. Bolhuis¹ and L. Abelnmann¹. *1. University of Twente, MESA+ Institute for Nanotechnology, Enschede, Netherlands*

Thermal Analysis of Water Cooled IPMSM Using Thermal Equivalent Circuit Network

Kyu-Seob Kim, Byeong-Hwa Lee, Jae-Woo Jung, Jung-Pyo Hong, Senior member, IEEE

Department of Automotive Engineering, Hanyang University, Seoul, 133-791, Korea

Recently, interior permanent synchronous motor (IPMSM) is applied to an integrated starter and generator (ISG) for hybrid electric vehicle. In a design of such motor, thermal analysis is necessary to maximize power density because loss is proportional to the power of motor. Therefore, cooling device as a heat sink is required internally. Generally, a cooling system designed by water jacket structure is widely used to the electric motor because it has several advantages which are simple structure and cooling effectiveness. In order to analyze the electric machine with water jacket cooling system, thermal equivalent network can be effective approach. This thermal equivalent network is composed to thermal resistance, heat source, and thermal capacitance considering conduction, convection, and radiation. Especially, modeling of cooling channel in the network is difficult aspect owing to modeling with flow of the coolant. In this paper, temperature prediction using thermal equivalent network is performed in the ISG which has water cooled system. Then, experiment is conducted to verify the thermal equivalent network.

Index Terms— Cooling channel, Heat transfer of convection, Integrated starter and generator, radiant heat, Thermal equivalent circuit network, Water jacket

I. INTRODUCTION

INTEREST IN interior permanent magnet synchronous motor (IPMSM) has been growing for a long time because high torque and wide speed range can be achieved by flux weakening of current vector control. Recently in the automotive area, many researchers have focused efforts on IPMSM to develop an integrated starter and generator (ISG) for hybrid electric vehicles [1].

According to demanding of IPMSM with high power density, computation of radiant heat using cooling system becomes important task in the research and development. Internal heat of electric motor can be released by cooling system and it can help to design the motor with high power density. In other words, if the heat is rapidly radiated to external coolant in the cooling system high power density will be obtained to use of high current density in even size [2].

The high performance of cooling method is divided by two parts such as water-cooled, and oil-cooled according to the material of coolant. Most of all, oil cooled type is the best method to radiate heat because it can be sprayed or sunk directly into the hotspot of armature winding. However, mechanical structure of these systems is too complicated to design. Secondly, the type of water cooled system can be designed by water jacket which is inserted a cooling channel between housing and stator. This type of system is widely applied to the electric motor because of its simple structure and cooling effectiveness. In this case, low temperature of coolant is going into inlet of external device and going out to the outlet with internal heat. Thus, temperature rising of motor caused by copper loss, core loss, and eddy current loss of PM can be minimized by such a cooling method. Finally, the motor is able to be operated continually despite of high current density.

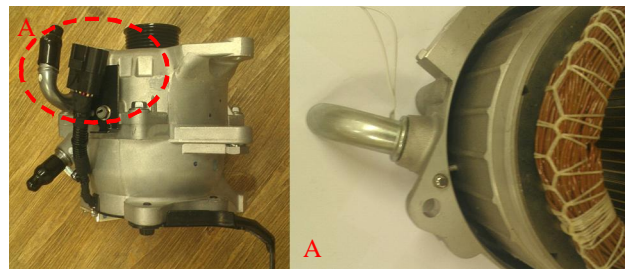


Fig. 1. Analysis model and cooling channel

The thermal equivalent network is one of method to predict temperature of electric motor. This method has been studied by many researchers. However, water cooled thermal equivalent network is more difficult because mathematical modeling for radiation of heat in the cooling channel is complicated. According to shape of water jacket, thermal equivalent network is composed by thermal resistance, thermal capacitance, and radiant heat. In this paper the motor temperature is estimated by thermal equivalent network and verifies by experiment.

II. HEAT TRANSFER OF WATER COOLED THERMAL EQUIVALENT CIRCUIT NETWORK

Fig.1 shows analysis model. Inlet and outlet of water jacket are confirmed to Fig.1, cooling channel is shown in the part A. The coolant flows through cooling channel which covers the stator surface.

In thermal equivalent circuit network, temperature rising is converted to voltage variation, motor loss is converted to current source. Convection and conduction are converted to thermal resistance, and thermal capacity is capacitance. This network in the water jacket is shown in Fig.2 considering heat flow. P_{WJ} is thermal resistance of coolant, C_{WJ} is thermal capacitance of coolant, R_{WJ} is thermal resistance of coolant, R_1 is thermal resistance of housing, and C_1 is thermal capacitance of housing. Parameters of cooling channel and housing are connected to internal circuit.

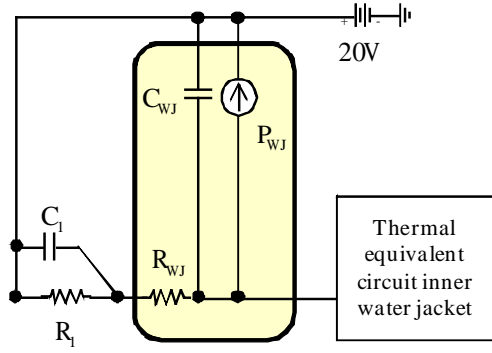


Fig. 2. Modeling of water jacket

A. Radiant heat by coolant

A coolant radiates heat as it flows along water jacket. Generally, losses are substituted with heat sources, which have positive values, in equivalent thermal circuit. On the contrary, radiation heat stands for the heat transmitted from the inside to the outside and has a negative value. As described in Fig. 2, P_{wj} is connected to a ground and it means that heat is radiated to external areas by means of coolant. Consequently, it is probable that a direction of radiation heat for coolant is determined and we assume an equivalent effect on which an actual coolant has.

Quantity of radiant heat is express by

$$P_{wj} = \dot{Q} \cdot dT \cdot \rho \cdot C_p \quad (1)$$

where q is flow rate of coolant, dt is difference between inlet and outlet, ρ is density of coolant, and C_p is specific heat.

That is, the quantity of radiation heat is relevant to the volume and the temperature change of coolant, and a thermal capacity as an ability that takes up heat in the equation (1). On the average, the flux of coolant used in cooling is 8~10 LPM. As well, the temperature range between an inlet and an outlet for coolant is roughly 2~3 °C. If the flow rate and difference temperature cannot be confirmed by external cooling system, this value is used.

B. Thermal resistance of coolant

The flow of the coolant according to cooling channel is defined to forced convection by water. In the convection, thermal resistance is derived by

$$R_{wj} = \frac{1}{hA} \quad (2)$$

where h is coefficient of heat transfer by forced convection, A is area through the coolant. Fig. 3 shows r-z section view included cooling channel which is located between housing and stator. In general the cooling channel is parted by one or several path, which has helical shape or even several parallel lines. In thermal equivalent circuit network, the study of heat transfer is a part which is a difficult analysis because of flow of coolant. However, forced convection is studied by field of fluid mechanics, the equation of convection is adopted by pipe flow. The flow of coolant is described by pipe flow. In [3], Nu ,

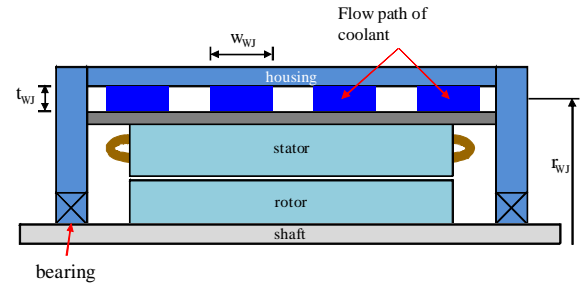


Fig. 3. r-z section view included cooling channel

Pr , and Re calculated by experimental method in the flow.

This experimental equation is derived by

$$Nu = \frac{f / 8 \times (Re - 1000) \times Pr}{1 + 12.7 \times (f / 8)^{0.5} \times (Pr^{2/3} - 1)} \quad (3)$$

$$f = [0.790 \times \ln(Re) - 1.64]^{-2} \quad (4)$$

where f is friction factor, Nu is the Nusselt number, Pr is the Prantl number, and Re is the Reynolds number. These dimensionless numbers are essential to analyze the fluid flow [4]. Especially, because Nu is related coefficient of heat transfer, h is computed by

$$h = Nu \times \frac{k}{D_h} \quad (5)$$

where k is thermal conductivity, D_h is characteristic length through flow of coolant.

Flow area of the coolant is calculated by

$$A = 2(t_{wj} + w_{wj}) \times (2\pi r_{wj}) \times n_{wj} \quad (6)$$

where t_{wj} is thickness, w_{wj} is width, and r_{wj} is length between center of motor and cooling channel, and n_{wj} is the number of cooling channel. Thermal resistance of cooling channel is calculated by coefficient of convection and flow area of coolant. Therefore, these parameters of the coolant have an effect on motor temperature in the steady state.

C. Thermal capacitance of coolant

The thermal capacity is expressed by capacitance. In other words, delaying the temperature change has a similar meaning with delaying voltage change. The thermal capacity is a product of mass and specific heat. Especially, specific heat can be categorized into 2 specific heats under constant volume and constant pressure and the former is being used in a driving mode of motor because of a constant volume of fluid. This is as follows.

$$C_{wj} = \rho C_p V \quad (7)$$

where ρ is density of coolant, C_p is specific heat, V is volume of coolant. Because the coolant flows continuously, volume of coolant is calculated in the cooling channel.

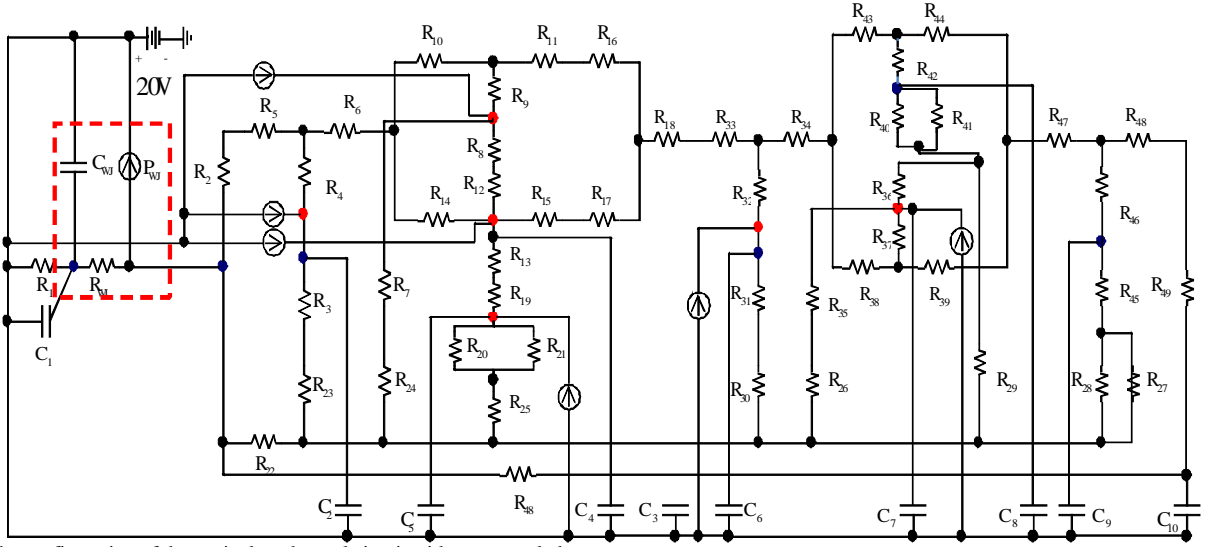


Fig. 4. The configuration of the equivalent thermal circuit with water-cooled system

III. COMPOSITION OF THERMAL EQUIVALENT CIRCUIT NETWORK

There exist a lot of similarities between the equivalent thermal circuits based on air-cooled and water-cooled systems. The only difference is that the outer surface of stator is directly connected to housing, or convection thermal resistance, in the former and an additional water jacket is attached with the same structure. Thus, the two interior configurations are almost identical. The Fig.4 describes the configuration of the equivalent thermal circuit with water-cooled system. The part marked as dotted line with the color “red” is relevant to the water jacket. As explained in II, it includes radiation heat, thermal resistance in the case of forced convection, and thermal capacitance. As well, the circuit for housing is shown in the left figure and that for stator and rotor in the right. Since a variety of researches for the interior equivalent thermal circuit has been performed, it is identically applied in this paper considering the model [5], [6]. Here, the thermal resistances in radial direction are allocated from the left to the right and the ones in axial direction from the upper to the lower. That is, the flow of heat is converted from three to two dimensions and so is precisely calculated.

IV. ANALYSIS MODEL AND THERMAL PARAMETER

The analysis model which is dealt with in this paper is motor for ISG. The ISG is emerging as a low-cost fuel-saving technology in vehicles. In addition to its conventional alternator functions, it fulfills some functional requirements of

TABLE I
SPECIFICATION OF ANALYSIS MODEL

	Unit	Value
Poles / slots	-	6 / 36
Dc link voltage	Vdc	-
Max. torque	Nm	-
Output power	kW	8
Max. speed	RPM	-
Size	mm	-

mild hybrid systems, including starting the stopped ICE, driving the vehicle when starting, driving the auxiliaries when the ICE is stopped, and regenerative braking. Supporting the ICE during acceleration is also possible with ISG technology. The power-flow control of fully hybridized PHEVs in this work will become a new application of ISGs [7].

The specification of electric machine is shown in table I. It has 6 poles/36 slots with distributed windings. Furthermore, it generates 23.5Nm and 8kW at the operating point, 3250 RPM. The size indicates the external diameter of stator.

As shown in Fig. 1, the exterior shape of the motor is so complex that it is not simple to determine the convection coefficients of air and housing when equivalent thermal circuit network is applied to. In contrast, since it is a water-cooled motor, the conditions of air and housing cannot have a strong influence on it. The other parts are similar to those of generic motors and so equivalent thermal circuit network is applicable. That is, because 2 major heat sources, copper loss and core loss, are positioned inside a cooling channel, the heat created is not transmitted to the outside. Also, the temperature of housing is almost same as that of cooling water and then the complexity of the exterior shape is not a problem in using equivalent thermal circuit network.

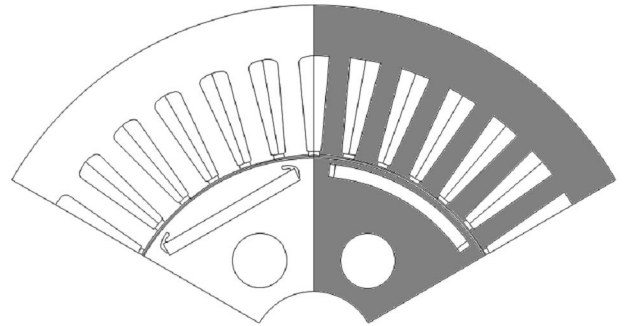


Fig. 5. The configuration of the analysis model

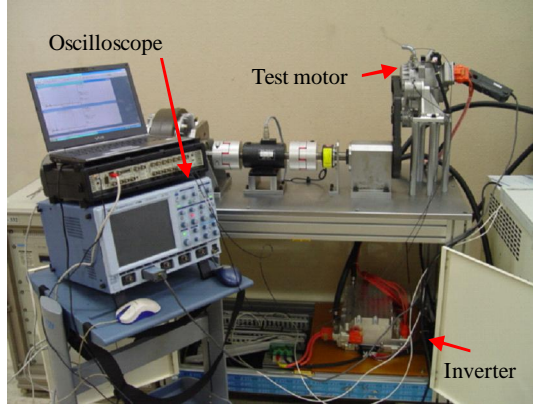


Fig. 6. Test set for thermal analysis

TABLE I
VALUE OF HEAT SOURCE

	Unit	Copper loss	Core loss		
			Yoke	Teeth	Rotor
Loss	W	669.6	27.3	29.4	6.3

The Fig.5 describes the configuration of the analysis model. The left shows the shape of actual model and the right the model needed to utilize equivalent thermal circuit network. Because it is based on the cylindrical model, the figures of slot, permanent magnet, and flux barrier are treated with the same areas.

The table I indicates the values of heat sources. The majority of total loss is copper loss whereas core loss is about 10% of copper loss. Thus, we can predict that the variation of temperature is mainly determined by the value of copper loss.

V. RESULT OF ANALYSIS AND THERMAL TEST

Temperature analysis and the corresponding experiment are performed. For analysis, the equivalent thermal model is needed and the condition is shown in Table II. The operating point is 3250 RPM and the load is 23.5Nm. To consider a actual condition, it is analyzed in a chamber whose temperature 105 °C. As well, the cooling water flows inside the motor and the temperature of its inlet is 70 °C while that of its outlet 72-73 °C.

As a result, we can confirm that the temperature of coil ranges from 70 °C to 139 °C. An experiment is performed to verify the results. The Fig.6 shows a test set used in the experiment. A thermal couple is attached to the end coil inside the motor to identify the temperature. Moreover, a dynamo is connected to the motor to inject the load and a torque meter to measure the value of torque.

The load test is carried out based on analysis condition. The result shows Fig.7 that the temperature of coil ranges from 70 °C to 134 °C. Therefore, the error between the analysis and the experiment is roughly 10%. Also, the similarity of the temperature's raising pattern is more important. Through the comparison between the results from the analysis and experiment, it is noticeable that they show an almost same aspect at early temperature.

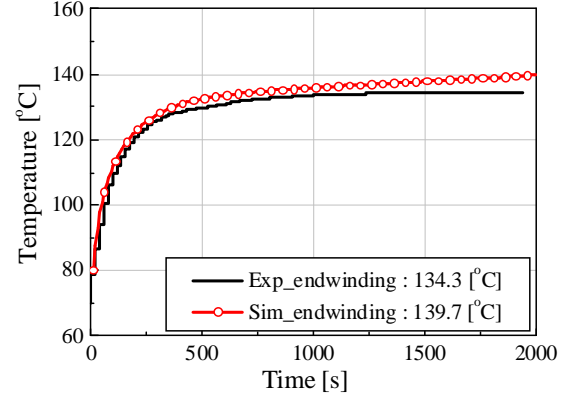


Fig. 7. Analysis and test result of thermal analysis

TABLE II
CONDITION OF ANALYSIS AND THERMAL TEST

	Unit	Value
Speed	RPM	3250
Torque	Nm	23.5
Power	kW	8
Chamber temperature	°C	105
Temperature of cooling channel	°C	70

VI. CONCLUSION

This paper formulates an equivalent thermal circuit network with water cooling system and verifies the results through an experiment. In the case of the model with water jacket, it is difficult to apply a heat analysis model of cooling channel to the motor and determine a convection coefficient because of the forced convection. Therefore, the circuit is made after the heat properties of fluid as cooling liquid is checked. The motor for HSG, which is used in experiment, has a complex shape of housing, but the cooling channel can be simplified as one channel which is applicable for experiment.

The conclusion is that it is possible to perform the temperature analysis and predict the thermal properties of the motor using the equivalent thermal circuit network at early design.

REFERENCES

- [1] Chai Feng, Pei Yulong, Li Xinmei, Guo Bin, and Cheng Shukang, "The Performance Research of Starter-Generator Based on Reluctance Torque Used in HEV," IEEE Trans. on Magn., vol. 45, no.1, pp. 635-638, 2009.
- [2] Jin Hur and Byeong-Woo Kim, "Rotor Shape Design of an Interior PM Type BLDC Motor for Improving Mechanical Vibration and EMI Characteristics," JEET, vol. 5, no. 3, pp.462-467, 2010.
- [3] V.Gnielinski, "New Equations for Heat and Mass Transfer in Turbulent Pipe and Channel Flow," American Institute of Chemical Engineer, vol. 16, no. 3, pp.359-368, 1961.
- [4] Yunus A. Cengel, Heat transfer: A practical approach, 2nd ed., McGraw-Hill, 2003.
- [5] P. H. Mellor, D. R. Roberts, D. Turner, "Lumped Parameter Thermal Model For Electrical Machines of TEFC Design," IEE, vol.138, no. 5, 1991.
- [6] Byeong-Hwa Lee, Kyu-Seob Kim, Jae-Woo Jung, Jung-Pyo Hong, and Young-Kyoun Kim, "Temperature estimation of IPMSM using thermal equivalent circuit," IEEE Trans. on Magn., to be published.
- [7] Sunil Adhikari, Saman K. Halgamuge, and Harry C. Watson, "An Online Power-Balancing Strategy for a Parallel Hybrid Electric Vehicle Assisted by an Integrated Starter Generator," IEEE Trans. on Vehicular Technology, vol. 59, no.6, pp. 2689-2699, 2010.